ORIGINAL PAPER

K. Shinoda · M. Yamakata · T. Nanba · H. Kimura
T. Moriwaki · Y. Kondo · T. Kawamoto · N. Niimi
N. Miyoshi · N. Aikawa

High-pressure phase transition and behavior of protons in brucite Mg(OH)₂: a high-pressure–temperature study using IR synchrotron radiation

Abstract Infrared absorption spectra of brucite $Mg(OH)_2$ were measured under high pressure and high temperature from 0.1 MPa 25 °C to 16 GPa 360 °C using infrared synchrotron radiation at BL43IR of Spring-8 and a high-temperature diamond-anvil cell. Brucite originally has an absorption peak at 3700 cm^{-1}, which is due to the OH dipole at ambient pressure. Over 3 GPa, brucite shows a pressure-induced absorption peak at 3650 cm^{-1}. The pressure-induced peak can be assigned to a new OH dipole under pressure. The new peak indicates that brucite has a new proton site under pressure and undergoes a high-pressure phase transition. From observations of the pressure-induced peak under various P–T condition, a stable region of the high-pressure phase was determined. The original peak shifts to lower wavenumber at −0.25 cm^{-1} GPa^{-1}, while the pressure-induced peak shifts at −5.1 cm^{-1} GPa^{-1}. These negative dependences of original and pressure-induced peak shifts against pressure result from enhanced hydrogen bond by shortened O–H···O distance, and the two dependences must result from the differences of hydrogen bond types of the original and pressure-induced peaks, most likely from trifurcated and bent types, respectively. Under high pressure and high temperature, the pressure-induced peak disappears, but a broad absorption band between 3300 and 3500 cm^{-1} was observed. The broad absorption band may suggest free proton, and the possibility of proton conduction in brucite under high pressure and temperature.

Keywords Brucite · Infrared synchrotron radiation (IRSR) · IR microspectroscopy · High-temperature diamond-anvil cell (HTDAC) · High-pressure phase transition · Proton transfer · SPring-8

K. Shinoda (✉) · N. Niimi · N. Miyoshi · N. Aikawa
Department of Geosciences,
Graduate School of Science,
Osaka City Univ.,
Osaka 558-8585, Japan
e-mail: shinoda@sci.osaka-cu.ac.jp
Tel.: +81-6-6605-3173; Fax: +81-6-6605-3174

M. Yamakata · H. Kimura · T. Moriwaki
Spring-8/JASRI, Mikazuki,
Hyogo 679-5198, Japan

T. Nanba
Graduate School of Science and Technology,
Kobe Univ., Kobe 657-8501, Japan

Y. Kondo
Department of Applied Physics,
Tohoku Univ.,
Sendai 980-8579 Japan

T. Kawamoto
Institute for Geothermal Sciences,
Kyoto Univ.,
Beppu 874-0903 Japan

Introduction

To investigate the influence of hydroxyls (OH) on the physical properties of minerals, it is an important experimental theme to observe directly the behavior of protons in hydrous silicate minerals and nominally anhydrous minerals under high temperature (HT) and high pressure (HP). Infrared (IR) spectroscopy is a proper method to detect OH in minerals. The HT diamond-anvil cell (HTDAC) is a widely used apparatus to study the physicochemical state of minerals under HT and HP. In this study, a newly constructed HTDAC was applied to IR microspectroscopy, and IR absorption spectra of brucite ($Mg(OH)_2$) were measured under HT and HP.

Recently, an IR synchrotron radiation (IRSR) beamline named BL43IR was constructed at synchrotron radiation facility SPring-8, Hyogo, Japan. IRSR as an IR light source has the advantages of a higher brilliance than conventional IR light source and a wide range of wavenumber from visible to far IR regions. Four experimental stations (Infrared Microspectroscopy, Surface Science, Absorption and Reflection Spectroscopy, and Magneto-optical Spectroscopy) are working for multiuses of IRSR

at BL43IR (Kimura H. et al. 2001). At the IR micro-spectroscopy station, an IR microscope was newly constructed for various micromeasurements of IR spectra on a region as small as 10 μm (Kimura S. et al. 2001). Figure 1 shows intensity mapping of IRSR and conventional IR sources between 1000 and 9000 cm^{-1} at the sample stage of the IR microscope of BL43IR (Matsunami et al. 2001). The IRSR is 100 times more brilliant than the conventional IR source, and is focused as a spot of FWHM 10 μm at the sample stage of the IR microscope. Although the usual measured spot with conventional micro-FTIR is about 100 μm ϕ, micro-IR measurements at the 10 μm ϕ area without aperture can usually be performed by the IR microscope of BL43IR. The IRSR is very useful for micromeasurements with space resolution 10 μm. The IR microscope of BL43IR has the advantage of a long working space, as large as 100 mm between Schwartzschild-type mirrors of x8 and NA (numerical aperture) 0.5, to capacitate voluminous apparatus such as a HTDAC, a LTDAC, a cryostat, and a mapping stage of 1-μm steps. The IR microscope can also perform in situ measurements of ruby fluorescence to determine pressure for DAC studies. As a small sample of 10 μm order is required to be confined in a gasket hole of 100 μm ϕ for HTDAC experiments, this system is useful for experimentally difficult measurements, such as HTDAC study.

The crystal structure of brucite is the CdI$_2$ ($P\bar{3}m1$) structure with MgO$_6$ octahedral layers (brucite layer) stacked along the c axis and the OH dipole oriented parallel to the c axis on a three-fold axis (Bragg and Claringbull 1965). The hydrogen bond between a hydroxyl on a brucite layer (donors OH) and an oxygen on the next layer (acceptors O′) is very weak, as evidenced by the (001) perfect cleavage. Whereas portlandite Ca(OH)$_2$, which is isomorphous with brucite, undergoes pressure-induced amorphization above 10 GPa (Meade et al. 1992), brucite does not transfer to an amorphous state on compression (Duffy et al. 1995a). Brucite is widely studied as a prototype of hydrous magnesium silicates, because Mg(OH)$_2$ is located at the middle point between MgO and H$_2$O in the MgO–SiO$_2$–H$_2$O system and is an end member of the binary system Mg(OH)$_2$–Mg$_2$SiO$_4$, where dense hydrous magnesium silicates Phase A and humite minerals are plotted. An X-ray study clearly showed no phase transition involving the Mg–O substructure under high pressure (Duffy et al. 1995a). Nagai et al. (2000) studied the compression mechanism of brucite by X-ray powder diffraction. Neutron diffraction studies of Mg(OD)$_2$ (Parise et al. 1994) and Mg(OH)$_2$ (Catti et al. 1995) indicated a possibility of disordered hydrogen bond between OH on a brucite layer and an oxygen (O′) on the next layer. Duffy et al. (1995b) suggested a pressure-induced phase transition in brucite by observing several new Raman spectroscopic peaks, but the structural change is unknown. Kruger et al. (1989) observed a pressure-induced IR absorption peak at 3650 cm^{-1} and assigned it to a hot band from the first excited state to the overtone. Although some possibilities of structural changes of OH in brucite had been proposed, a clear view of any phase transition was not clear. Shinoda and Aikawa (1998) also observed a pressure-induced absorption peak at 3650 cm^{-1} with DAC and polarized IR spectroscopy, and assigned it to a new OH dipole formed by proton transfer between donor OH and nearest-neighbor acceptor O′ under pressure. Figure 2 shows a schematic figure of a new proton site of brucite under pressure as proposed by Shinoda and Aikawa (1998). The original OH dipole is represented by O–H, and the pressure-induced one is O′–H′. The original OH dipole is normal to the brucite layer and the proton is coordinated to three nearest-neighbor oxygens. The pressure-induced O′H′ dipole is inclined to the c axis and coordinated to one oxygen which originally formed the donors' OH. Since the O′–H′ dipole is randomly formed between donor OH and the three nearest-neighbor acceptor O′, the distribution of O′–H′ dipoles is trigonally disordered over a crystal. In this study, IR absorption spectra of brucite were measured under various P–T conditions with HTDAC and IRSR. The possibility of a high-pressure phase transition of brucite and its stable region are discussed.

Fig. 1 Intensity mapping of IRSR and conventional IR (globar) sources between 1000 and 9000 cm^{-1} by scanning 2 μm ϕ pinhole at 1 μm steps at the sample stage of the IR microscope at BL43IR of SPring-8. The *vertical axis* of the conventional IR source is enlarged 25 times. (Matsunami et al. 2001)
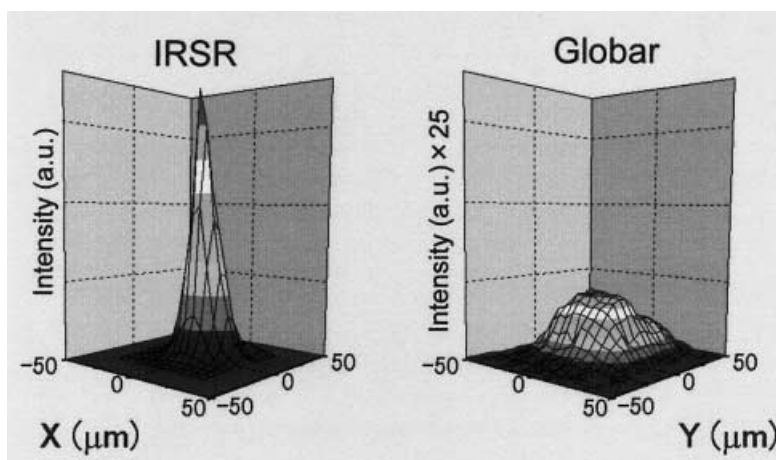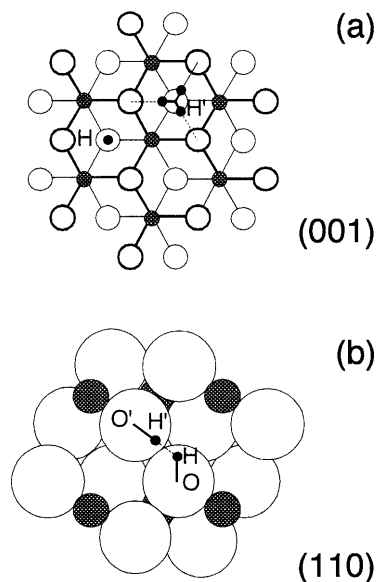
Fig. 2a, b Schematic crystal structure of brucite. Hydroxyls and Mg atoms are represented as *open* and *filled circles*. **a** A (001) view of brucite layer, where upper and lower hydroxyls are *thick* and *thin lines*, respectively. **b** A (110) horizontal view of layers. The original OH dipole is vertical to a brucite layer, and represented as O–H dipole. The O′–H′ dipole indicates a pressure-induced OH dipole in brucite. (Shinoda and Aikawa 1998)

Experimental

Figure 3 schematically shows the lever-type and externally heating HTDAC under the IR microscope of BL43IR. The HTDAC is settled on a pulse stage of 1 μm steps. The ruby fluorescence technique was used for measuring pressure at elevated temperature (Piermarini et al. 1975; Ragan et al. 1992). A thermocouple located by the diamond was used for measuring temperature. A Ia-type diamond of 2.2 mm height and 0.5 mm ϕ culet was used. Fluorocarbon fluid (Fluorinert, 3M Company) was used as pressure medium. Rhenium foil of 250 μm thickness preindented and drilled into 200 μm ϕ with a YAG 1064-nm laser was used as a gasket. IR spectra were measured at 20 μm diameter with an LN_2 cooled InSb detector and Bruker FTIR IFS 120 HR with a KBr beam splitter under the condition of 4 cm^{-1} resolution and 512 scans. A natural clear single crystal of brucite from Zimbabwe and a reagent grade $Mg(OH)_2$ powder sample were prepared for HTDAC study. A (001) oriented platelet of brucite of 50 μm square was made by the perfect cleavage of the natural sample. Powdered natural brucite and reagent $Mg(OH)_2$ samples were mixed with KBr powder, and KBr pellets with 10 wt% $Mg(OH)_2$ were formed. Reference spectra were measured at the empty place in the gasket. Two series of experiments using the (001) platelet sample were carried out. *P–T* conditions of the experiments using the (001) platelet sample are shown in Fig. 4, where circles and squares show measured points of IR spectra and arrows indicate the *P–T* path of experiments. The sample was pressurized by the lever at 25 °C, and no further pressure was applied by the lever during heating of the sample. Because of thermal expansion of pressure medium, internal pressure increased by heating without further pressuring.

Results and discussion

Figure 5a shows IR absorption spectra of (001) platelet single crystal of brucite from 0.1 MPa, 25 °C to
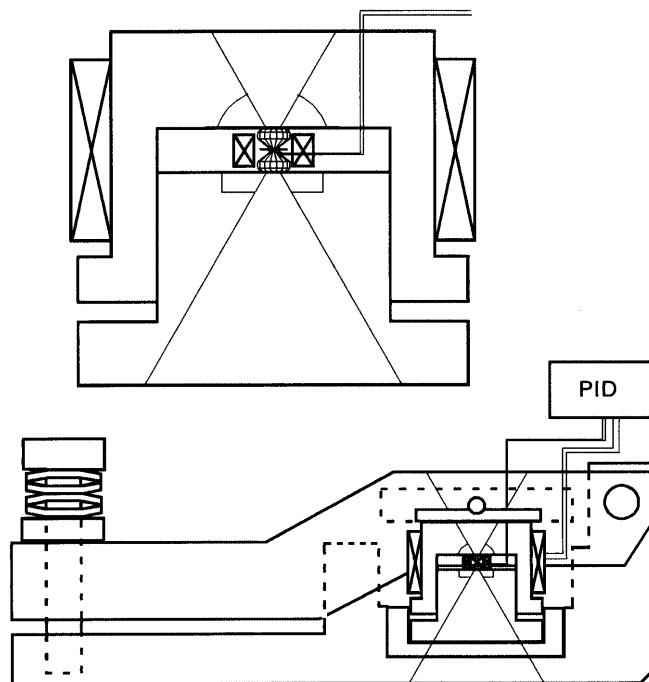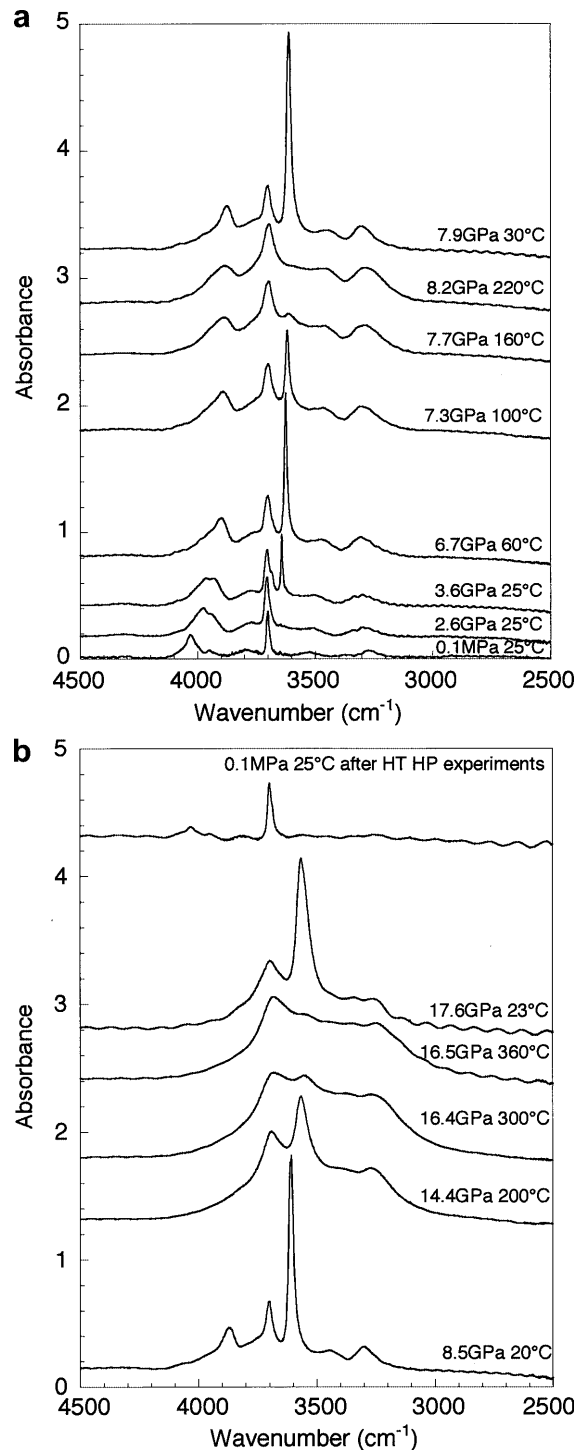

Fig. 3 A schematic figure of a lever-type and externally heating HT DAC of BL43IR of Spring-8. Piston and cylinder parts are conically cut at an angle of 60°, which is consistent with angle of NA of Schwartzschild mirrors of the IR microscope. The top and bottom of the piston and cylinder parts are thermally insulated by zirconia ceramics. An electric resistance heater surrounds the cylinder part and a thermocouple is placed in contact with diamonds. The heater and the thermocouple are joined to a PID-type controller and electric source

8.2 GPa, 220 °C. An absorption peak of the original OH dipole is observed at 3700 cm^{-1} under 0.1 MPa, 25 °C. A pressure-induced absorption peak (PI peak) appeared at 3650 cm^{-1} over 3 GPa at 25 °C. Two peaks around 4000 and 3300 cm^{-1} can be assigned to enhanced overtone or combination band due to the Mg–O bond, which is characteristic of single crystal because the two peaks are not observed in powdered sample. The sample was pressurized up to 3.6 GPa and heated. Absorbance of the PI peak increased on compression and decreased on heating. The peak position of the PI peak shifted to a lower wavenumber on compression. On heating, the PI peak continued to be observed at 7.7 GPa, 160 °C, and disappeared at 8.2 GPa, 200 °C. After cooling, internal pressure remained at 7.9 GPa and the intense PI peak appeared again. Figure 5b shows IR absorption spectra up to 16.5 GPa, 360 °C. In the higher-pressure region, the PI peak was observed to the higher temperatures. The PI peak can be observed under 320 °C, 16.3 GPa, and disappeared at 340 °C, 16.0 GPa. After cooling, pressure remained at 17.6 GPa and the intense PI peak appeared again (17.6 GPa, 23 °C). After depressurizing, the PI peak disappeared and the original peak still remained. These observations indicate that the onset of the PI peak is a reversible and unquenchable phenomenon. As proposed by Shinoda and Aikawa (1998), we
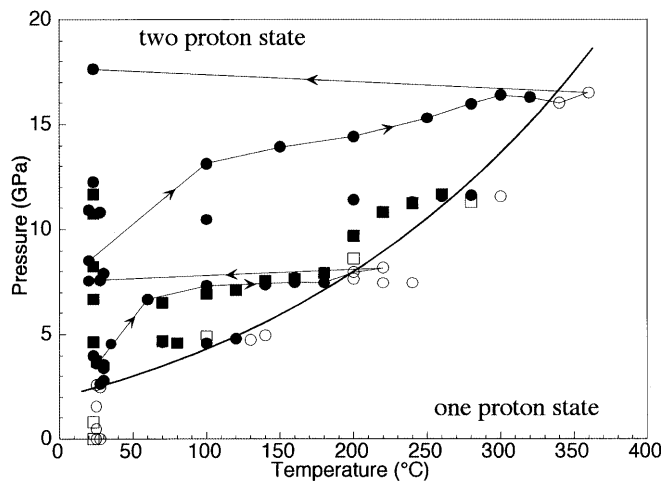
Fig. 4 Measured points of IR absorption spectra in this study. *Circles* and *squares* represent two series of HT and HP experiments with (001) platelet single crystals of brucite. *Two thin lines and arrows* represent the P–T paths of IR spectra in Fig. 5a, b. The points where the PI peak was observed are represented by *filled symbols* and *open symbols* are no PI peak. A *thick line* indicates a boundary between an open and a filled mark. This indicates a phase boundary of brucite between two-proton and one-proton states

Fig. 5a, b IR absorption spectra of (001) platelet single crystal of natural brucite from Zimbabwe up to 8.2 GPa 220 °C (**a**), and 16.5 GPa 360 °C (**b**). An absorption peak at 3700 cm^{-1} is due to the original OH-stretching motion and the PI peak appears in the lower wavenumber side of the original. The sample was heated until the PI peak disappears. Over 16 GPa 300 °C, the PI peak become weak, but a broad band between 3300 and 3600 cm^{-1} grows

consider that the onset of the PI peak indicates the formation of a new OH dipole in brucite under pressure and that this high-pressure phase transition involves a new proton site. No phase transition involving the Mg–O substructure is assumed here as indicated by Duffy et al. (1995a). The formation process of the new OH dipole can be proton transfer between brucite layers. At ambient pressure, there is no interaction between OH in a brucite layer and O′ of the next layer. By compression, the O···O′ distance is shortened, and the energy levels of two neighboring OH groups overlap (Freund 1967; Martens and Freund 1976). The activation energy of proton transfer to the adjacent oxygen is lowered by shortening O···O′ distance and proton transfer is enhanced, and the resultant O′H′ dipole is formed. (Fig. 2). The O′H′ dipole must be inclined to the c axis from the pleochroism of polarized IR absorbance (Shinoda and Aikawa 1998). Under the higher temperature, the proportion of a vibrational state in the first excited state must be increased. If the PI peak is a hot band due to a transition from the first excited state to the overtone, as proposed by Kruger et al. (1989), absorption of the PI peak would be increased by heating. However, absorption of the PI peak decreases under higher temperature. This implies that the PI peak is not a hot band but a newly formed OH dipole under pressure. According to neutron diffraction studies of Mg(OD)$_2$ (Parise et al. 1994) and Mg(OH)$_2$ (Catti et al. 1995), H/D undergoes disorder transition between OD/OH and one of the three neighboring O′. D/H disorder means that a proton on the threefold axis at ambient pressure approaches one of the three neighboring O′ under compression; as a result, protons randomly occupy three off-axis H or D sites. This is based on gradual widening

of the OHO′ angle observed by the neutron diffraction studies. Our results also suggest inclined and randomly trifurcated O′H dipoles under compression, and

furthermore, we suggest a clear view of transition that the O'H dipole is not gradually formed by shortening of the OHO' distance, but is discretely formed by the proton's occupancy of a new site. In Fig. 4, filled circles and squares show the presence of the PI peak, and open ones show no PI peak. Therefore, the boundary between the open and filled marks in Fig. 4 can be a phase boundary of brucite. The state of the two protons is stable in the high-pressure region.

The original OH dipoles in brucite are oriented parallel to the c axis. When absorption spectra of the (001) plate of brucite are measured, the original OH dipoles in brucite are normal to the electric vector of IR light ($\mathbf{E} \perp \mathbf{c}$). This condition results in inactive IR absorption for the original OH dipoles of brucite. Thus, absorption of the original peak is only weakly observed in Fig. 5. On the other hand, absorption of the PI peak was confirmed to be maximized under $\mathbf{E} \perp \mathbf{c}$ by polarized IR study with DAC (Shinoda and Aikawa 1998), so absorption of the PI peak is intensely observed in Fig. 5. The (001) single-crystal platelet is the most sensitive sample to confirm the presence or absence of the PI peak. Because of the orientation relation of original and PI peaks against IR absorption, the relative intensity of the two peaks in Fig. 5 does not indicate the actual proportion of the proton's occupancy of original and PI sites. The actual proportion of the PI peak to the original peak can be estimated by the powdered samples. Figure 6 shows IR absorption spectra of fragments of KBr pellet of natural (Fig. 6A) and reagent (Fig. 6B) powdered $Mg(OH)_2$. As shown by peak height in Fig. 6, the ratio of the original and the PI OH is about 2:1 at 9.1 GPa and 30 °C. The proportion of the PI peak increases under the higher pressure region.

Figure 7 shows the wavenumber shift of original (open) and PI (filled) peaks against pressure at 25, 100, 200, and 300 °C. The original peak shows weak negative dependence of -0.25 cm^{-1} GPa^{-1}. The PI peak shows an intense negative dependence of -5.1 cm^{-1} GPa^{-1}. In general, the wavenumber of the OH-stretching absorption is an index of the strength of hydrogen bond or O–H···O' distance. The wavenumber shifts to lower frequency by enhanced hydrogen bond or shortened O–H···O' distance (Nakamoto et al. 1955). The negative dependences of original and PI peaks must result from enhanced hydrogen bonding caused by shortening O–H···O' distance under compression. However, weak and intense negative dependence of wavenumber position cannot be simply explained by enhanced hydrogen bond. Nakamoto et al. (1955) classified the hydrogen bond into three types, that is, straight, bent, and bifurcated hydrogen bonds. They also indicated that the bent hydrogen bond shows a higher wavenumber shift than the straight one. On the other hand, the bifurcated one has a lower shift than the straight one. So, the bent-type hydrogen bond generally shows a much higher wavenumber shift than the bifurcated type. We propose that the PI O'H' dipole is formed by proton transfer along the H···O' direction, as shown in Fig. 2. According to this
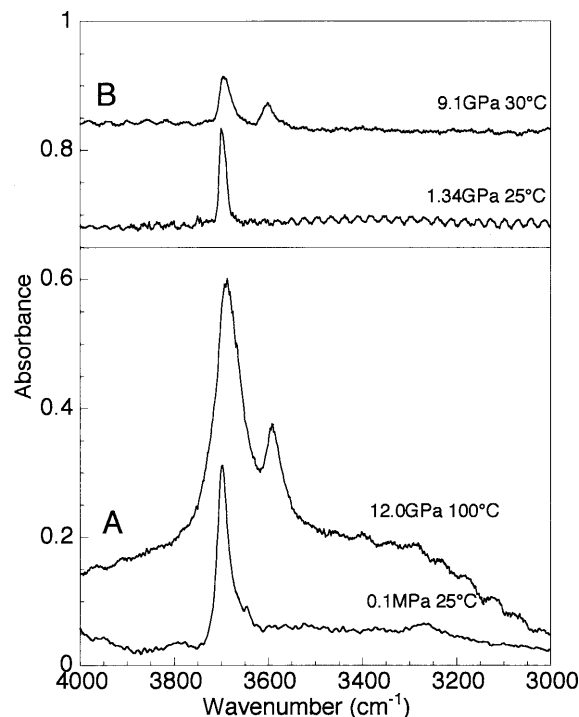
Fig. 6A, B IR absorption spectra of powdered $Mg(OH)_2$ pellet [10 wt% $Mg(OH)_2$ and KBr] of Zimbabwe (**A**) and reagent (**B**). Compared with the spectrum of the (001) single crystal under similar conditions (Fig. 5a 7.9 GPa 30 °C), the PI peak of powdered sample is not so intense as the spectra of the (001) single crystal. Since powdered samples are randomly oriented crystal, the relative intensity of original and PI peaks represents the proportion of protons on original and new proton sites

model, the O···H'–O' geometry is a bent-type hydrogen bond. On the other hand, the geometry of the original OH is trifurcated type, because the original OH dipole remains on the threefold axis and H is coordinated to three nearest-neighbor O'. Since the wavenumber shift of the bent hydrogen bond is generally expected to be higher than that of the bifurcated hydrogen bond, the PI OH dipole of the bent hydrogen bond should show a higher wavenumber shift than the original OH with a trifurcated hydrogen-bond type. The two different peak shifts of the original and the PI peak in Fig. 7 can be qualitatively explained by the general relation of wavenumber shift and classification of hydrogen bond. Thus, these results also support the formation of a new proton site under pressure.

The PI peak becomes weak in the high-pressure and high-temperature region, but a broad absorption band between 3300 and 3600 cm^{-1} grows, as is clearly seen in the spectrum at 16.5 GPa, 360 °C in Fig. 5b. Since Fei and Mao (1993) indicated that $Mg(OH)_2$ is stable as the brucite phase at 16.5 GPa, 360 °C in the MgO–H_2O system, the broad band must not indicate the formation of H_2O molecules accompanied by the decomposition of brucite. Since brucite does not undergo pressure-induced amorphization as portlandite $Ca(OH)_2$ does, the broad band must not indicate the amorphous state of
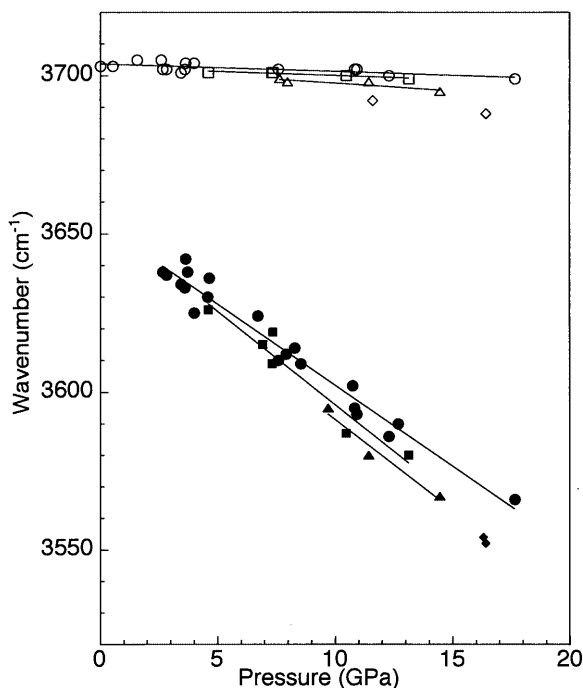
Fig. 7 The wavenumber position of the original (*open*) and the PI (*filled*) peaks against pressure (● RT: ■ 100 °C; ▲ 200 °C; ◆ 300 °C). Pressure dependence of the original peak at RT is −0.25 cm^{-1} GPa^{-1} and the PI is −5.1 cm^{-1} GPa^{-1}. The peak position depends mainly on pressure and slightly on temperature

$Mg(OH)_2$ as the IR absorption spectra of portlandite does (Shinoda et al. 2000). Although the Mg–O-related peak at 3300 cm^{-1} slightly broadens in the high-temperature region in Fig. 5b, the contributing area of this band to the broad band between 3300 and 3600 cm^{-1} is small. Therefore, it can be assumed that the broad band indicates a proton state which does not occupy a specific crystallographic site under HT and HP. This means that OH dipoles occupy various sites, which cause sequential absorption wavenumber. Thus, the broad absorption band may suggest that free protons occur in brucite and that brucite may transform into a proton-conductive state under HT and HP. The transfer process of proton, which is limited to proton transfer at low temperature, may proceed to thermally activated transfer of protons at HT and HP.

Concluding remarks

Brucite undergoes a high-pressure phase transition from one-proton to two-proton states under high pressure, as shown by the onset of PI peak. Brucite has a new proton site in the high-pressure phase. The region of the high-pressure phase was determined by the presence and absence of the PI peak under various *P–T* conditions. Two different pressure dependences of wavenumber shift of original and PI peaks result from the hydrogen bond of trifurcated and bent types, respectively. These support the model of the new proton site under high pressure. A broad absorption band between 3300 and 3600 cm^{-1} in IR absorption spectra of brucite may suggest the possibility of proton conduction of brucite under high temperature and high pressure.

References

Bragg L, Claringbull GF (1965) Crystal structure of minerals. In: Sir Lawrence Bragg (ed) The crystalline state, vol. 4, G. Bell and Sons, Ltd London

Catti M, Ferraris G, Hull S, Pavese A (1995) Static compression and H disorder in brucite, $Mg(OH)_2$, to 11 GPa: a powder neutron diffraction study. Phys Chem Miner 22: 200–206

Duffy TS, Shu J, Mao HK, Hemley RJ (1995a) Single-crystal X-ray diffraction of brucite to 14 GPa. Phys Chem Miner 22: 277–281

Duffy TS, Meade C, Fei Y, Mao HK, Hemley RJ (1995b) High-pressure phase transition in brucite, $Mg(OH)_2$. Am Mineral 80: 222–230

Fei Y, Mao HK (1993) Static compression of $Mg(OH)_2$ to 78 GPa at high temperature and constraints on the equation of state of fluid H_2O. J Geophys Res 98: 11875–11884

Freund F (1967) Retention of hydroxyl groups on magnesium oxide. J Am Ceram Soc 50: 493–494

Kimura H, Moriwaki T, Takahashi S, Aoyagi H, Matsushita T, Ishizawa Y, Masaki M, Oishi S, Ohkuma H, Namba T, Sakurai M, Kimura S, Okamura H, Nakagawa N, Takahashi T, Fukui K, Shinoda K, Kondoh Y, Sata T, Okuno M, Matsunami M, Koyanagi R, Yoshimatsu Y, Ishikawa T (2001) Infrared beamline BL43IR at SPring-8: design and commissioning. Nucl Instrum Meth (A) 441–444

Kimura S, Nanba T, Sada T, Okuno M, Matsunami M, Shinoda K, Kimura H, Moriwaki T, Yamakata M, Kondo Y, Yoshimatsu Y, Takahashi T, Fukui K, Kawamoto T, Ishikawa T (2001) Infrared spectromicroscopy and magneto-optical imaging stations at SPring-8. Nucl Instrum Meth (A) 893–896

Kruger MB, Williams Q, Jeanloz R (1989) Vibrational spectra of $Mg(OH)_2$ and $Ca(OH)_2$ under pressure. J Chem Phys 91: 5910–5915

Mao HK, Xu J, Bell PM (1986) Calibration of the ruby pressure gauge to 800 kbar under quasi-hydrostatic condition. J Geophys Res 91: 4673–4676

Martens R, Freund F (1976) The potential energy curve of the proton and the dissociation energy of the OH$^-$ ion in $Mg(OH)_2$. Phys Stat Sol (a) 37: 97–104

Matsunami M, Sada T, Chen L, Nanba T, Shinoda K, Kondo Y, Kawamoto T, Kimura H, Moriwaki T, Ikemoto Y, Yamakata T (2001) Spectromicroscopy by highly brilliant infrared synchrotron radiation. Abstract no.18a PS-9 Annual Meeting Physical Society of Japan, Tokushima

Meade C, Jeanloz R, Hemley RJ (1992) Spectroscopic and X-ray diffraction studies of metastable crystalline-amorphous transition in $Ca(OH)_2$ and serpentine. In: Syono Y, Manghnani MH (eds) High-pressure research: application to Earth and planetary sciences, Terra Scientific, Tokyo, pp 485–492

Nakamoto K, Margoshes M, Rundle RE (1955) Stretching frequencies as a function of distances in hydrogen bond. J Am Chem Soc 77: 6480–6486

Nagai T, Hattori T, Yamanaka T (2000) Compression mechanism of brucite: an investigation by structural refinement under pressure. Am Mineral 85: 760–764

Parise JB, Leinenweber K, Weidner DJ, Tan K, Von Dreele RB (1994) Pressure-induced H bonding: neutron diffraction study of brucite, $Mg(OD)_2$, to 9.3 GPa. Am Mineral 79: 193–196

Piermarini GJ, Block S, Barnett JD, Forman RA (1975) Calibration of the pressure dependence of the R1 ruby fluorescence line to 195 kbar. J Appl Phys 46: 2774–2780

Ragan DD, Gustavsen R, Schiferl D (1992) Calibration of the ruby R1 and R2 fluorescence shifts as a function of temperature from 0 to 600 K. J Appl Phys 72: 5539–5544

Shinoda K, Aikawa N (1998) Interlayer proton transfer in brucite under pressure by polarized IR spectroscopy to 5.3 GPa. Phys Chem Miner 25: 197–202

Shinoda K, Nagai T, Aikawa N (2000) Pressure-dependent anharmonic coefficient of OH in portlandite by NIR–IR spectroscopy with DAC. J Miner Petrol Sci 95: 65–70